

Mesons a in Collinear QCD Model

M. Burkardt

Department of Physics
New Mexico State University
Las Cruces, NM 88003-0001
U.S.A.

A phenomenological model for the quark structure of mesons is considered. The model is based on the tube model for QCD, where all quanta with nonzero transverse momenta are neglected. In the limit that the mass term of the gluons goes to infinity, the model is equivalent to a combination of the 't Hooft and Gross-Neveu models and can be solved semi-analytically. The model has the properties of confinement, chiral symmetry breaking and asymptotic freedom and thus resembles QCD in three key respects. Spectra, distribution amplitudes and form factors of mesons are analyzed.

I. INTRODUCTION

Many high energy scattering processes, probe the quark-gluon structure of hadrons predominantly in one direction [1]. It is thus suggestive to consider a phenomenological model for QCD, where the transverse momenta of all constituents are neglected. At a semi-classical level, one can think of this approximation as a formulation of QCD in a "tube" with periodic boundary conditions. By taking the radius of the tube very small, all modes other than $\vec{k}_\perp = 0$ have a very high energy and thus freeze out. The model which will be considered in this work is based on such a classical reduction of the QCD Lagrangian to an effective 1+1 dimensional theory, which is subsequently quantized. It should be emphasized that the model thus obtained is not a dimensional reduction at the level of the full quantum theory, which is slightly more subtle. As a consequence, the model should not be considered a rigorous approximation to full QCD but rather a phenomenological model. Furthermore, it should be noted that even though the model is formulated in 1+1 dimensions, one should not consider it a mere toy model but rather a simple (because all \vec{k}_\perp vanish) phenomenological model for QCD_{3+1} .

While it may be possible to understand many features of high energy scattering experiments in terms of a simplified effective theory, which is reduced to degrees of freedom with vanishing transverse momenta, boost invariance often seems essential for microscopic descriptions of such experiments. Furthermore, high energy scattering experiments typically probe correlations along light-like directions [1]. It thus makes sense to employ light-front (LF) quantization [2-5] when studying dimensionally reduced QCD.

Such a model has been considered in Ref. [6] for glue-balls and in Ref. [7] for mesons, where discrete light-cone

quantization (DLCQ) [8] has been used as a numerical tool. However, due to the rather singular behavior of the fermion wave functions, the resulting spectra are not very well converged numerically when the quark masses become small. For form factors, which we would like to consider in this work, it is even more important to describe the end-point behavior of the wave functions very accurately. Improvement methods based on DLCQ [9] have so far only been developed for gluons.

In order to develop a model which can be solved semi-analytically, we will consider a modified version of the model in Ref. [7] where we assume that the mass term for the effective gluon is very large and thus gluon degrees of freedom can be eliminated perturbatively. The resulting effective interaction for the quarks resembles 't Hooft's large- N_c QCD in 1+1 dimensions [10] with an additional helicity dependent Gross-Neveu interaction [11,12].

Because the matter degrees of freedom in collinear QCD couple to a 1+1 dimensional gauge theory, confinement is an almost trivial feature of the model. The effective Gross-Neveu interaction, which arises from eliminating the transverse gluons, provides an induced mass for the quarks and thus leads to spontaneous breaking of chiral symmetry. Furthermore, the Gross-Neveu interaction is also asymptotically free. Thus, even though collinear QCD cannot be derived rigorously as an approximation to full QCD, the mere fact that it shares with real QCD the important properties of confinement, chiral symmetry breaking as well as asymptotic freedom makes it worth while to investigate collinear QCD as a phenomenological model.

As a first application of the model, we will study the low lying meson spectrum. This part of the calculation will also be used to determine the free parameters of the model. Once all terms in the Hamiltonian are fixed, we will then proceed to calculate other observables, specifically distribution amplitudes (i.e. light-cone wave functions) and form factors.

II. THE COLLINEAR QCD MODEL FOR MESONS

The basic idea of collinear QCD (also referred to as the tube model) is to start from the classical QCD Lagrangian and to neglect all dependences on transverse coordinates (transverse with respect to an arbitrarily chosen, but fixed direction), yielding

$$\mathcal{L} = \bar{\psi} \left[\gamma^+ (i\partial_+ - gA_+) + \gamma^- (i\partial_- - gA_-) - g\vec{\gamma}_\perp \vec{A}_\perp - m \right] \psi - \frac{1}{2} \text{tr} G^{\mu\nu} G_{\mu\nu} - \frac{\lambda^2}{2} \vec{A}_\perp^2, \quad (2.1)$$

where we have introduced LF coordinates $A_\mp = A^\pm = (A^0 \pm A^3)$. To keep the calculations simple, which will help in identifying the essential physics, only the limit $N_c \rightarrow \infty$ will be considered here.

Neglecting modes with $\vec{k}_\perp \neq 0$ breaks invariance under \vec{x}_\perp dependent gauge transformations. Therefore a mass for the transverse component of the gauge field has been added, since it is now no longer protected by gauge invariance. Eq. (2.1) is still invariant under gauge transformations that depend on x^\pm only and we are thus free to choose the gauge $A^+ = 0$.¹ Neither A^- nor ψ_\pm (where $\psi_\pm \equiv \frac{1}{2}\gamma^\mp\gamma^\pm\psi$) are dynamical degrees of freedom, since their LF-time (x^+) derivative does not enter the Lagrangian (2.1). This degrees of freedom are eliminated from the Lagrangian [Eq. (2.1)] using the corresponding constraint equations (Euler Lagrange equations) before quantizing the theory.

The dynamical degrees of freedom of the model are ψ_+ and \vec{A}_\perp , which are quantized canonically. In summary, what the dimensional reduction yields is a 1+1 dimensional gauge theory, coupled to both scalar matter in the adjoint representation (\vec{A}_\perp) and fermionic matter in the fundamental representation (ψ). Both \vec{A}_\perp and ψ have internal helicity degrees of freedom — remnants of the underlying 3+1 dimensional theory.

In addition to the coupling of the matter fields to the 1+1 dimensional gauge theory, there is also a direct, Yukawa-like, coupling between fermions and \vec{A}_\perp , which flips the helicity of the fermions.

Note that the dimensional reduction procedure, the choice of gauge ($A^+ = 0$) as well as the quantization plane ($x^+ = 0$) are all manifestly invariant under rotations about the z -axis. As a result, the z -component of the total angular momentum is a conserved quantity in the model. Since there is no orbital angular momentum left after the dimensional reduction, this means that the total z -component of the spin, i.e. the sums of z -components of the spins of quarks, plus anti-quarks plus gluons, is conserved. This feature of the model will be very helpful when it comes to classifying states.

Such a model has been studied in Ref. [7], where approximate numerical solutions have been obtained using a Fock space expansion and DLCQ [8]. In Ref. [7], one can also find an explicit expression for the dimensionally reduced LF Hamiltonian for QCD, which will not be reproduced here in its full generality, since we will consider only a solvable limiting case of the model in this work.

By allowing the mass term for \vec{A}_\perp to become arbitrarily large (with appropriate rescaling of the coupling constant in order to keep the physics nontrivial), it is possible to systematically eliminate \vec{A}_\perp , yielding an effective interaction which acts only on the fermion degrees of freedom. For this we note that, as long as they are not diverging, all interactions of \vec{A}_\perp become negligible in this limit. Furthermore, we can neglect all interactions in intermediate states which contain quanta of \vec{A}_\perp and are thus highly off-shell. This makes it an easy task to eliminate \vec{A}_\perp using a LF Tamm-Danoff procedure. First this gives rise to a kinetic mass counter-term for the fermions. As is explained in the Appendix, the Tamm-Danoff procedure also requires to renormalize the one gluon vertex. After eliminating all gluon dressing from the quark lines, we are thus left with a fermion field that has a mass term M .²

In order to determine the effective $q\bar{q}$ interaction arising from eliminating \vec{A}_\perp , let us consider $q\bar{q}$ scattering (Fig. 1)³

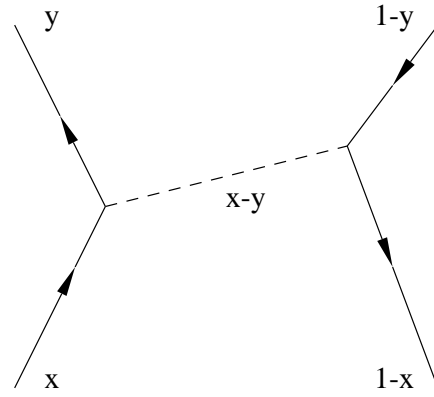


FIG. 1. Scattering of a quark with initial LF-momentum x from an anti-quark of initial momentum $1 - x$. The dotted line represents the exchanged gluon. Only one time ordering is shown.

Since the quark helicity flips at the quark gluon vertices and since total (quark+gluon) helicity is conserved at each vertex, the one gluon exchange interaction vanishes identically for helicity ± 1 mesons, i.e. when quark and antiquark have the same helicity. Thus, as our first result, we find that mesons with helicity ± 1 are in our model described by 't Hooft's equation only

¹Explicit zero-modes, i.e. modes that do not depend on x^- , will be neglected throughout this work.

²Strictly speaking we would have to keep separate kinetic and vertex mass terms. However, as is discussed in Appendix A, choosing them equal gives rise to a consistent solution.

³Once again, since $\lambda \rightarrow \infty$, all other interactions can be neglected in intermediate states with \vec{A}_\perp quanta.

$$\tilde{\mu}_n^2 \psi(x) = \left(\frac{M^2}{x} + \frac{M^2}{1-x} \right) \psi(x) + G^2 \int_0^1 dy \frac{\psi(x) - \psi(y)}{(x-y)^2}. \quad (2.2)$$

The only role played by the transverse gluons for these mesons is to give the quarks a “constituent mass” M .

The situation is different for mesons with helicity zero, i.e. when quark and antiquark have opposite helicity, in which case the one gluon exchange matrix element is nonzero and reads for the time ordering depicted in Fig. 1⁴

$$\begin{aligned} \langle x | V_{oge}^{Fig.1} | y \rangle &\propto \frac{g^2 \frac{\Theta(x-y)}{x-y} \left(\frac{1}{x} - \frac{1}{y} \right) \left(\frac{1}{1-x} - \frac{1}{1-y} \right)}{2P^+P^- - \frac{M^2}{y} - \frac{M^2}{1-x} - \frac{\lambda^2}{x-y}} \\ &\xrightarrow{\lambda^2 \rightarrow \infty} \frac{-g^2 \Theta(x-y) \left(\frac{1}{x} - \frac{1}{y} \right) \left(\frac{1}{1-x} - \frac{1}{1-y} \right)}{\lambda^2} \end{aligned} \quad (2.3)$$

The other time-ordering gives (for $\lambda \rightarrow \infty$) the same expression, but with $\Theta(y-x)$, so that the Θ -function disappears in the sum of the two time-orderings

$$\begin{aligned} \langle x | V_{oge} | y \rangle &\propto \frac{-g^2}{2\lambda^2} \left[\left(\frac{1}{x} + \frac{1}{1-x} \right) \left(\frac{1}{y} + \frac{1}{1-y} \right) \right. \\ &\quad + \left(\frac{1}{x} - \frac{1}{1-x} \right) \left(\frac{1}{y} - \frac{1}{1-y} \right) \\ &\quad \left. + \frac{2}{x(1-x)} + \frac{2}{y(1-y)} \right], \end{aligned} \quad (2.4)$$

where the different Lorentz structures appearing in Eq. (2.3) have been separated. Let us first consider the “pion” channel, i.e. mesons with helicity zero, an odd spin wave function and an even orbital wave function for the quarks. In this channel, the effective interaction reads

$$\begin{aligned} \langle x | V_{oge}^{eff,\pi} | y \rangle &\propto \frac{-g_{eff}^2}{2} \left[\left(\frac{1}{x} + \frac{1}{1-x} \right) \left(\frac{1}{y} + \frac{1}{1-y} \right) \right. \\ &\quad \left. + \frac{2}{x(1-x)} + \frac{2}{y(1-y)} \right] \end{aligned} \quad (2.5)$$

where $g_{eff}^2 = g^2/\lambda^2$. The first interaction term in Eq. (2.5) is the same as what one gets in the chiral Gross-Neveu model, i.e. an attractive s-channel $\bar{\psi}_i i\gamma_5 \psi_i \bar{\psi}_j i\gamma_5 \psi_j$ interaction, where i, j are color indices. Such an interaction leads to a divergence when it is iterated and one has to introduce a cutoff. From studies of the Gross-Neveu model [11,12], it is known that the coupling g_{eff} goes to zero as the cutoff is sent to infinity (asymptotic freedom!). The other two terms in Eq. (2.5) are what one

gets if one introduces an s-channel vector interaction of the form $\bar{\psi}_i \gamma_\mu \psi_i \bar{\psi}_j \gamma^\mu \psi_j$ in $1+1$ dimensions. Such an interaction does not lead to divergences (in covariant perturbation theory) — neither when iterated with itself nor in conjunction with the QCD_{1+1} or Gross-Neveu interactions. Thus as the running coupling goes to zero, this s-channel vector interaction becomes less and less important, until it disappears when the cutoff goes to infinity. In the effective interaction, one can thus omit this term entirely, yielding

$$\langle x | V_{oge}^{eff,\pi} | y \rangle \propto \frac{-g_{eff}^2}{2} \left(\frac{1}{x} + \frac{1}{1-x} \right) \left(\frac{1}{y} + \frac{1}{1-y} \right). \quad (2.6)$$

In the scalar channel (total helicity zero, spin part odd, orbital part odd) one finds the same result as for the chiral Gross-Neveu model in the scalar channel

$$\langle x | V_{oge}^{eff,\sigma} | y \rangle \propto \frac{-g_{eff}^2}{2} \left(\frac{1}{x} - \frac{1}{1-x} \right) \left(\frac{1}{y} - \frac{1}{1-y} \right) \quad (2.7)$$

and also the relative sign and strength between the π and σ channel are consistent with the chiral Gross-Neveu model.

In addition to this contact interaction from eliminating the transverse Gluon field, the mesons are also governed by the QCD_{1+1} interactions. Thus, after all the dust has settled, we are left with an effective two dimensional field theory, describing mesons both in the π and σ channels, which in covariant notation reads⁵

$$\begin{aligned} \mathcal{L} = \bar{\psi} \left(i\partial - \frac{G}{\sqrt{N}} A - m \right) \psi - \frac{1}{2} \text{tr} (F_{\mu\nu} F^{\mu\nu}) \\ - \frac{\gamma}{2N} \left[(\bar{\psi} \psi)^2 - (\bar{\psi} i\gamma_5 \psi)^2 \right], \end{aligned} \quad (2.8)$$

where ψ is a two-spinor with N color components (fundamental representation), $F_{\mu\nu} = \partial_\mu A_\nu - \partial_\nu A_\mu + i\frac{G}{\sqrt{N}} [A_\mu, A_\nu]$ is the gauge field and the limit $N \rightarrow \infty$ is implied. Obviously, for $\gamma = 0$ one obtains the 't Hooft model (QCD_{1+1} in the limit $N \rightarrow \infty$) [10],

Finally, let us turn to mesons with zero total helicity, but even helicity wave functions. By the same reasoning as above, one obtains the same interaction as in the $\pi - \sigma$ channels, but with the sign reversed (because the interaction is a spin exchange interaction), i.e. they act repulsively. In non-perturbative calculations, there is a crucial difference between renormalized zero-range interactions that are attractive and those that are repulsive! This fact is best illustrated in the context of a simple example, the

⁴ The overall coupling is irrelevant at this point, since it is renormalized anyways.

⁵ One can arrive at the same result also by means of a rather lengthy Fierz rearrangement. However, it is much more illuminating to derive this result in the LF helicity basis as has been done above.

non-relativistic Schrödinger equation in two spatial dimensions with a delta function interaction. Since a delta function in two dimensions leads to a logarithmic divergence, one needs to introduce a cutoff. Suppose now that the delta function is attractive. Then, in order to keep a finite mass of the bound state, the coupling constant must go to zero as the cutoff goes to infinity — otherwise the wave-function gets sucked into the singularity. Now suppose one calculates the effect of a repulsive interaction with the same strength but opposite (repulsive) sign. In this case, there is no enhancement of the interaction due to being sucked in and as a consequence the repulsive effects of the interaction completely disappear as the cutoff is sent to infinity.

The same happens here with the spin-even helicity zero interaction. Because of the symmetries of the underlying action, the coupling constant is the same as in the attractive case ($\pi - \sigma$ channel) but of opposite (repulsive) sign. Since non-perturbative renormalization for the $\pi - \sigma$ channel (as done in Appendix B) yields a vanishing bare coupling, and since the same bare coupling acts in the repulsive case, one finds that the effective interaction from one gluon exchange in the repulsive channels completely disappears. The spin-even helicity 0 mesons are thus described by 't Hooft's equation (without Gross-Neveu interaction). This is a very interesting result, since it implies that the spin-even helicity 0 mesons are described by the same bound-state equation as the helicity ± 1 mesons, and they thus form degenerate triplets — just as one would expect from vector and axial vector mesons!

In summary, after separating the spin part of the effective interaction induced by the transverse gluons, one finds that scalar and pseudo-scalar mesons are described by the 't Hooft – Gross – Neveu interaction [Eq. (2.8)], while vector and axial vector mesons are described by 't Hooft's equation [Eq. (2.8), but with $\gamma = 0$].⁶ This is one of the principal results of this paper.

Quantum numbers are associated with these states by considering vacuum to meson matrix elements of operators with definite quantum numbers (such as $\psi\psi$ and $\bar{\psi}i\gamma_5\psi$). The resulting quantum numbers are consistent with the quantum numbers that one can intuitively guess by merely considering the degeneracy of states and their naive quark model parity properties. Using these rules, one obtains the assignments of quantum numbers shown in Table I. Of course, while the above assignment of quantum numbers may appear reasonable, it is still to some extend arbitrary, since the model has no rotational symmetry. One should always keep this fact in mind when

comparing the model results to the experimentally measured meson spectra.

Note that, in the limit of infinite mass for the A_\perp field considered here, the model supports only states with helicity up to $h = 1$. Tensor and higher spin mesons are absent in this limit of the model.

helicity	hel. symmetry	orbital symmetry	J^P
0	odd	odd	0^+
0	odd	even	0^-
0	even	odd	1^+
1	even	odd	1^+
0	even	even	1^-
1	even	even	1^-

TABLE I. Assignment of J^P quantum numbers to the states of the model. One of the remarkable results of this model is that, despite the rotationally non-invariant formulation, states with $h = 0$ and those with $h = \pm 1$ are exactly degenerate (this is true for both vector and axial vector mesons).

⁶However, the effective masses of the quarks in the vector and axial vector channels are the same as the ones generated by the Gross-Neveu interactions in the scalar and pseudo-scalar channels.

III. NUMERICAL RESULTS

A. Meson Spectrum

In the case of vector and axial vector mesons, the numerical calculations amount to just solving 't Hooft's equation, which has been well studied and nothing further needs to be said about this part. For the scalar and pseudo-scalar mesons, which are described by a combination of the 't Hooft and Gross-Neveu models, the calculational methods to obtain spectra and wave functions are described in the Appendix B. In both cases (i.e. with and without Gross-Neveu interaction) the numerical calculations were based on variational calculations with a basis of Jacobi polynomials, such that the correct endpoint behavior of the wave functions was manifestly built in. typically, a basis size of 5-10 states was already sufficient to give the lowest eigenvalues with at least four significant digits.

The model contains three free parameters: the QCD_{1+1} coupling, the Gross-Neveu coupling and the effective (constituent) quark mass. These parameters were fixed by using as input the masses of the π , ρ and $\rho(1450)$ mesons. The masses of both the ρ and the $\rho(1450)$ do not depend on the Gross-Neveu coupling, and they thus determine the values of the bare parameters in the QCD_{1+1} interactions, yielding $m_q = 288\text{MeV}$ and $\sqrt{G^2/\pi} = 278\text{MeV}$ respectively.⁷ The value of the renormalized Gross-Neveu coupling is then obtained by performing a subtraction at the π pole as explained in Appendix B.

The physical string tension can be read off directly from the static $Q\bar{Q}$ potential in QCD_{1+1}

$$V(x) = \frac{G^2}{2}|x|. \quad (3.1)$$

For the above model parameters, one thus obtains a physical string tension of $\sigma = (349\text{MeV})^2$, which is slightly lower than the preferred value used by the lattice community [$\sigma_{latt} \approx (400\text{MeV})^2$].

Having determined all free parameters, we can now turn to calculate masses of other hadrons. When comparing with experimental data, the comparison is always done with isospin one states. The reason for this choice is that the model makes a large N_c approximation, and it is generally expected that such an approximation is better for isospin one states than for isospin zero states, since isospin zero states in QCD are affected by mixing with gluonic components and such mixing is turned off in the large N_c limit. Nevertheless, identifying the model

spectrum with isospin 1 states is still to some extend an arbitrary choice.

Numerical results for the lightest mesons and their first radial excitations are shown in Table II. Given the simplicity of the model, the agreement with the experimental data [14] is spectacular!

One may argue which of the mesons in Table II should be used as input parameters, particularly since some of these states are not believed to be simple quark model states but rather complicated "molecule" type states and one would not expect that such mesons are adequately described by a large N_c model. However, since all mesons in Table II are fitted quite well, picking a different set of input parameters has only a minor impact on the quality of the fit.

However, and this is more important, as we discussed in the previous session, there is the issue of assignment of quantum numbers, which reflects itself here in picking states from the particle data table [14] and comparing the model results to this data. Because of the truncation of transverse momenta, the model has less degrees of freedom than QCD (or a 3+1 dimensional quark model). Therefore, not all mesons with spin 0 or 1 have a model equivalent. By making (somewhat arbitrary) assignments of quantum numbers, one does in essence pick a subset of mesons from the particle data table and fits these mesons. As an example, the way we assigned quantum numbers, there are a_0 and b_1 mesons in the model but no a_1 mesons. In principle, one might thus be tempted to generate a fit to a different sub-set of mesons. However, since the above choice of quantum numbers seemed to be by far the most reasonable choice, no such results will be presented here. Nevertheless, one could always keep this in mind as an option.

meson	J^P	model (MeV)	exp.(MeV)
π	0^-	139 (input)	139
ρ	1^-	769 (input)	769 ± 1
a_0	0^+	978	984 ± 1
b_1	1^+	1249	1231 ± 10
$\pi(1300)$	0^-	1339	1300 ± 100
$\rho(1450)$	1^-	1465 (input)	1465 ± 25
a_0^*	0^+	1606 ± 2	?
b_1^*	1^+	1707	?

TABLE II. Calculated masses of the lightest mesons and their first radial excitations for each quantum number. Uncertainties are indicated only when they exceeded 1 MeV.

Motivated by the unexpected success of the model for calculations of the meson spectrum, we will in the following consider other observables as well. Of course, because of the severe approximations used in constructing the model, we will limit ourselves to observables where one would expect that the truncation of transverse momenta is not so critical. Furthermore, we will focus on those observables where the LF formalism is helpful in simplifying the calculations.

⁷Note that this quark mass includes already the mass renormalization due to the Gross-Neveu interactions and should thus be regarded as a constituent quark mass.

B. Meson Wave Functions

One quantity of great interest, which is easily accessible in our model, is the so called (twist-2) light-cone wave function of mesons, defined by a correlator along a light-like direction, i.e. for example

$$\psi_\pi(z) \propto \int d^2x dx^- \langle 0 | \bar{\psi}(0, x_\perp) \gamma^+ \gamma_5 \psi(x^-, x_\perp) | \pi \rangle e^{ip^+ x^- z} \quad (3.2)$$

in the case of the π , and correspondingly for the ρ . In gauges other than the LF-gauge $A^+ = 0$, a gauge string in Eq. (3.2) is understood. LF time x^+ is the same for the two field operators. Since the definition of these LF wave functions involves only longitudinal correlations, it seems sensible to consider them in our collinear model.

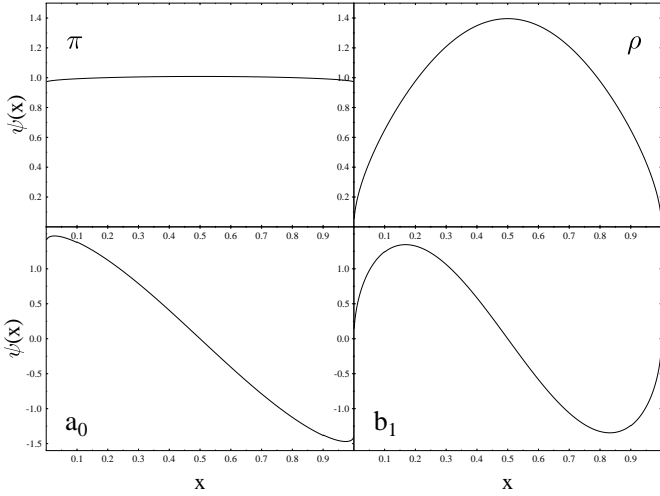


FIG. 2. Light-cone wave functions for the 4 lightest mesons.

Numerical results for the LF wave functions of the four lightest mesons are shown in Fig. 2. The wave functions for the π and ρ are normalized to f_π and f_ρ respectively, since this is common in discussions of these mesons. No such physically motivated normalization exists for the a_0 and b_1 mesons and they are thus normalized to $\int_0^1 dx \psi^2(x) = 1$. The ρ and b_1 are just solutions to 't Hooft's equation. The boundary behavior ($x \rightarrow 0, 1$) is $\psi \sim x^\beta [(1-x)^\beta]$, where $\pi\beta \cot \pi\beta = 1 - m_q^2 \pi/G^2$ and the number of nodes in the wave function increases with the excitation energy of the corresponding meson.

Obviously, this a crude model and one should be careful when comparing these results with other calculations or with experimental data. In particular, since modes with large transverse momenta have been omitted, one should only compare to calculations or data at a low momentum scale. With these caveats in mind, Fig. 2 shows several interesting features, which might be relevant for the real world. First of all, the pion wave function is nearly flat and it does not vanish at the end-points. This

is not just a numerical coincidence, as one can see by studying vacuum to meson matrix elements of the color singlet axial current

$$f_n p^\mu = \langle 0 | j_5^\mu | n \rangle. \quad (3.3)$$

In the chiral limit, $\partial_\mu j_5^\mu = 0$ and thus f_n must vanish — unless $\mu_n^2 = 0$. Only massless mesons are allowed to have $f_n \neq 0$ in the chiral limit. In terms of the LF wave functions,

$$f_n = \sqrt{\frac{N_C}{\pi}} \int_0^1 dx \phi_n(x) \quad (3.4)$$

and thus (regardless of the quark mass)

$$\frac{\pi}{N_C} \sum_n f_n^2 = 1. \quad (3.5)$$

If the π is the only massless meson in the chiral limit (it is in this model), then Eq. (3.5) implies

$$\int_0^1 dx \phi_\pi(x) = 1, \quad (3.6)$$

which, together with the normalization condition $\int_0^1 dx \phi_\pi^2(x) = 1$ and the Cauchy-Schwarz inequality, implies $\phi_\pi(x) = 1$, i.e. a constant π wave function. It should be emphasized that this argument does not work in more than 1+1 dimensions, where one also has to integrate over \vec{k}_\perp . However, in any 1+1 dimensional model with chiral symmetry and with only one massless meson state the wave function of this state must be flat. This statement holds even in the presence of higher Fock components, in which case one can also prove that (again if there is only one massless meson state) its wave function must be purely valence and flat.

The ρ meson wave function is peaked in the middle and it does vanish at the end points. The main reasons for the difference between the π and ρ meson wave functions are the stronger binding and the attractive short range interaction, which acts only in the pion channel. In a non-relativistic Schrödinger picture, the main difference between the π and the ρ is that the π wave function gets completely "sucked" into the region of the attractive short range interaction, thus leading to very high momentum components its wave function. End-points of the wave function on the LF, correspond to high momenta in an equal time picture, which explains why the π wave function is much larger than the ρ wave function near the kinematical end-points ($x = 0$ and $x = 1$).

Scalar and axial vector mesons show similar features as the π and ρ respectively, except that there is a node in the wave function, which arises since these mesons are simply the second lowest states in infinite ladders of states with an increasing number of nodes — very much similar to non-relativistic states in one space dimension. The reason for the difference between the end-point behavior of the a_0 and b_1 wave functions is the same as for the π and ρ .

Note that parton distribution functions in this model are simply the squares of the distribution amplitudes in this model, both because higher Fock components are negligible and because there are no integrals over transverse momenta. However, before comparing the resulting parton distributions with experimentally measured structure functions, one should bear in mind that the collinear approximation, i.e. neglecting quanta with $\vec{k}_\perp \neq 0$, makes sense only at low scales. Since it was not clear how to determine the starting scale for QCD evolution within the model, no attempt was made to compare the resulting structure functions to the available experimental data.

C. Meson Form Factors

In the case of the ρ meson, the 3 diagrams depicted in Fig. 3 contribute to the elastic form factor. As a side remark, it should be emphasized that in the LF framework, one can usually calculate form factors directly by taking matrix elements between the states and one does not need to worry about various diagrams (at least for the “good” component j^+ of the current). However, in the large N_C limit, the bound state equations are greatly simplified by leaving out all components of the wave function that are $1/N_C$ suppressed. On the LF this not only eliminates non-planar diagrams, but also diagrams which are planar but which contains fermion lines that go forth and back in time. When one calculates form factors, there are diagrams where the photon couples to such backward going lines, which become suddenly allowed, even on the LF, as long as the $+$ component of the momentum transfer is nonzero. Examples of such diagrams are shown in Fig. 3 b) and c).

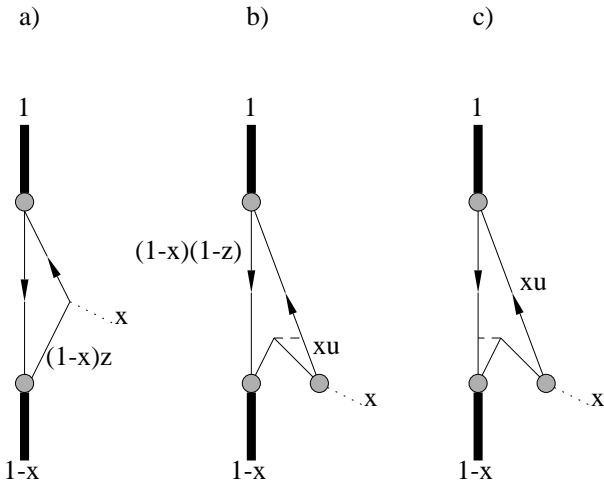


FIG. 3. Time ordered diagrams contributing to the vector form factor of the ρ meson: a) impulse term, b) vertex correction, c) exchange current. The grey blobs represents the meson wave function and the dressed quark photon vertex.

The expression for the elastic form factor of the ρ meson is identical to the corresponding expression for mesons in QCD_2 [13]. The reason is that the Gross-Neveu interaction neither contributes to the equation for the ρ nor does it contribute to the interaction in the photon (vector current!) channel. The form factor for mesons in QCD_2 has been derived in Ref. [13]

$$F^+ \equiv (2p^+ - q^+) F(q^2) = 2p^+ (1-x) [f^{imp} + f^{vc} + f^{ec}], \quad (3.7)$$

where $x = q^+ / p^+$,

$$f^{imp} = \int_0^1 dz \phi(x + (1-x)z) \phi(z) \quad (3.8)$$

is the “impulse term” (Fig. 3a),

$$f^{vc} = -x^2 G^2 \int_0^1 du \int_0^1 dz \frac{\phi(x + (1-x)z) \phi(z) G(u; q^2)}{[x(1-u) + (1-x)z]^2} \quad (3.9)$$

corresponds to a “vertex-correction” term (Fig. 3b), and

$$f^{ec} = x^2 G^2 \int_0^1 du \int_0^1 dz \frac{\phi(xu) \phi(z) G(u; q^2)}{[x(1-u) + (1-x)z]^2} \quad (3.10)$$

is the “exchange current” (Fig. 3c). $G(u; q^2)$ is the integrated Green’s function in QCD_2

$$G(u; q^2) = \int_0^1 dv G(u, v; q^2) \quad (3.11)$$

$$G(u, v; q^2) = \sum_n \frac{\phi_n(u) \phi_n(v)}{q^2 - \mu_n^2}.$$

The fraction $x \equiv q^+ / p^+$ of momentum transfer is determined by energy conservation

$$\mu^2 = \frac{q^2}{x} + \frac{\mu^2}{1-x}. \quad (3.12)$$

In the case of the π form factor, the same diagrams contribute, but there are two additional diagrams which contain backward moving lines that connect to the meson via a Gross-Neveu interaction (Fig. 4)

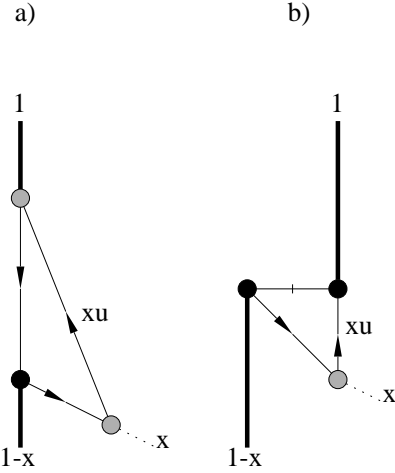


FIG. 4. Additional time ordered diagrams contributing to the vector form factor of the π . The grey blob represents the meson wave function as the dressed quark photon vertex, and the black blob the coupling of a quark to the meson via the Gross-Neveu interaction. The slashed fermion line corresponds to an instantaneous fermion exchange interaction.

The contribution of these diagrams to F^+ [Eq. (3.7)], the matrix element of j^+ is given by

$$Fig.4a = 2p^+x^2Z \int_0^1 du \left[\frac{M^2}{1-xu} - \frac{M^2}{x(1-u)} \right] \phi(xu)G(u; q^2) \quad (3.13)$$

and

$$Fig.4b = -2p^+x^2Z^2 \int_0^1 du \frac{M^2}{1-xu} G(u; q^2), \quad (3.14)$$

where Z is a constant related to the normalization of the vertex. Its value can be determined from

$$\phi(x) = -Z \int dy G(x, y, \mu^2) \frac{M^2}{y(1-y)}, \quad (3.15)$$

where ϕ is normalized according to $\int_0^1 dx \phi^2(x) = 1$.

In general, the wave functions and the integrals that determine the form factor [Eqs. (3.8)-(3.14)] have to be obtained numerically. However, in the chiral limit the pion wave function is constant $\phi_\pi(x) = 1$. This yields $f^{imp} = 1$. Furthermore, f^{vc} and f^{ec} exactly cancel each other. Finally, since $Z = 1$ in this case, there is also a partial cancelation between the two diagrams in Fig. 4, yielding

$$Fig.4 = -p^+x \int_0^1 du \frac{M^2}{1-u} G(u; q^2) = p^+x \left[1 - q^2 \int_0^1 du G(u; q^2) \right], \quad (3.16)$$

where we used that the solutions to 't Hooft's equation satisfy $M^2 \int_0^1 du \phi_n(u)/u(1-u) = \tilde{\mu}_n^2 \int_0^1 du \phi_n(u)$.

Adding up the various pieces and using furthermore [from Eq. (3.12)] that $q^+ = p^+$ (i.e. $x = 1$) for vanishing π mass, we thus find the remarkably simple result for the elastic vector form factor of the pion

$$F_\pi(q^2) = 1 - q^2 \int_0^1 du G(u; q^2) = \sum_n \frac{\tilde{\mu}_n^2 g_n^V}{\tilde{\mu}_n^2 - q^2}, \quad (3.17)$$

where $g_V(n) = \int_0^1 du \phi_n(u)$. In particular, we find for the rms-radius⁸

$$\langle r^2 \rangle = -6 \frac{d}{dq^2} F(q^2) = 6 \sum_n \frac{g_V(n)^2}{\tilde{\mu}_n^2}, \quad (3.18)$$

i.e. for the parameters used above one obtains a numerical value of

$$\sqrt{\langle r^2 \rangle_\pi} \approx 0.605 \text{ fm}, \quad (3.19)$$

which is only slightly smaller than the rms-radius for the ρ meson in the same model $\sqrt{\langle r^2 \rangle_\pi} \approx 0.625$. The explanation for this near equality of rms radii is that both form factors are dominated by the rho meson pole (note that $\sqrt{6}/m_\rho = 0.627 \text{ fm}$).⁹ The experimental value for the rms-radius of the pion is only slightly larger $\sqrt{\langle r^2 \rangle_{\pi,exp}} = 0.663 \pm 0.006 \text{ fm}$. However, one should not be too impressed by this excellent agreement, since the ρ mass is an input parameter and since the rms radius of the pion is dominated by the ρ meson pole. The interesting aspect of the model in this respect is that it reproduces vector meson dominance.

While the form factors of the π and ρ mesons are rather similar for low momentum transfers, there is a qualitative difference between them at large momentum transfers. The elastic form factor of the ρ meson follows the asymptotic behavior of form factors in QCD_2 , which is given by

$$F_\rho(Q^2) \sim \frac{1}{(Q^2)^{1+\beta}} \quad (Q^2 \rightarrow \infty), \quad (3.20)$$

where β is the same exponent that also appears in the end point behavior of the wave function. For the parameters used in the present fit ($m_q^2 \approx G^2/\pi$) one finds $\beta \approx 0.5$.

Naively, from Eq. (3.17) one would expect $F_\pi(Q^2) \sim 1/Q^2$ as predicted by naive power counting. However, $\sum_n \tilde{\mu}_n^2 g_P(n) g_V(n)$ diverges logarithmically and a more careful analysis yields

$$F_\pi(Q^2) \longrightarrow 2M^2 \frac{\ln Q^2}{Q^2} \quad (Q^2 \rightarrow \infty). \quad (3.21)$$

⁸Note that we use here the 3+1 dimensional relation between the slope of the form factor and the rms radius since this is supposed to be a model for 3+1 dimensional QCD.

⁹Of course, for the ρ meson it would be the ω meson pole, but in the large N_C limit the ρ and *omega* mesons are degenerate.

This logarithmic growth of $Q^2 F_\pi(Q^2)$ arises because we considered the limit of an infinitely heavy gluon in the collinear QCD model. One should thus not take Eq. (3.21) literally at very large Q^2 , but only in an intermediate momentum range, where it makes sense to introduce an infinitely heavy gluon as an effective degree of freedom.

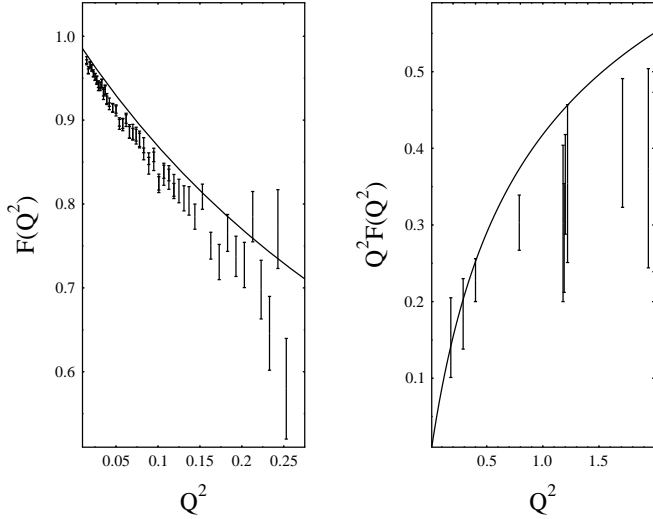


FIG. 5. Numerical results for the pion form factor [Eq. (3.17)]. The experimental data is from Ref. [15].

While the details of the form factor analysis at large Q^2 are model dependent, there are again some qualitative features which might be important also in full QCD_{3+1} . Since there is an attractive short range interaction acting only in the π channel, the wave function of the π (in an equal time picture) contains much more high momentum components than the ρ . As a result, the elastic form factor of the π should fall off much slower than the form factor of the ρ .

D. Strange Quarks

The extension of the model to include strange quarks is straightforward and any details will be omitted here. The only issue are the numerical values of the model parameters, i.e. which of the parameters one should take from the non-strange fit.

One might argue that the only new parameter is the strange quark mass, since the gauge coupling is obviously flavor independent and since the Gross-Neveu coupling also turns out to be flavor independent if one starts from a flavor independent coupling of the quarks to the transverse component of the gluons and if one strictly takes the limit of infinite mass for the transverse gluons. The results of a fit, where m_s as the only new parameter is shown in Table III. Using the K mass as an input, one finds $m_s = 502\text{MeV}$, which is quite heavy compared to a light quark mass of $m_q = 278\text{MeV}$ (the fitted value

from the non-strange sector). As a result, the masses of the K^* and the ϕ turn out to be much too high. Alternatively, if one uses the K^* mass as an input parameter,¹⁰ the K turns out much too light.

However, one should keep in mind that one should consider the Gross-Neveu interaction of the model an effective interaction, which is obtained by integrating out high energy degrees of freedom. In real QCD, these degrees of freedom do not have infinite mass and one would therefore expect some scale (and thus also some flavor-) dependence of the effective interaction. Since we are not able to perform this elimination procedure explicitly, we must also regard the Gross-Neveu coupling for strange quarks as an independent parameter in this phenomenological model. Corresponding results are shown in the forth column of Table III (fit 2). The strange quark mass in this case (from fitting the mass of the K^+) turns out to be $m_s = 408\text{MeV}$, which is much more reasonable compared to m_q than the above fit. The K mass is fitted by construction and yields the subtraction constant for the Gross-Neveu interaction,¹¹ which we used to calculate the mass of the lightest strange meson with 0^+ quantum numbers. Compared with the lightest meson with these quantum numbers that can be found in the particle data table, the model calculation gives a much too small mass. This is to some extend surprising, since the model did so well for the non-strange 0^+ meson. However, we will not attempt to explain this discrepancy here, since the quark model of these meson is to some extend still very speculative [16].

meson	J^P	fit 1	fit 2	exp.(MeV)
K^+	0^-	494 ± 5	494	494
K^*	1^-	986	892	892
ϕ	1^-	1198	1012	1020
$K^*(1430)$	0^+	1180 ± 10	1129	1429 ± 6

TABLE III. Comparison of numerically calculated meson masses to experimental data. In fit 1, all parameters other than the strange quark mass are taken from the non-strange fit. The Kaon mass is taken as an input parameter. In fit 2, the Gross-Neveu coupling is also allowed to differ from the coupling in the non-strange sector.

¹⁰Both the K^* and the ϕ do not depend on the Gross-Neveu coupling and are thus better suited for determining the strange quark mass independently from the Gross-Neveu coupling.

¹¹In fit 1 in Table III, the numerical results for the K and the $K^*(1430)$ have large errors associated with them, since those calculations do not subtract at the K -pole and one therefore has to deal numerically with divergent quantities.

The light-cone wave functions for mesons containing strange quarks are quite similar to wave functions of non-strange mesons and there is thus no reason to display them here. The only difference is that the wave-functions are no longer symmetric under $x \rightarrow 1 - x$, but they are slightly shifted such that the s quark tends to carry more momentum than the light quark, as one would naively expect.

One might also consider calculating form-factors of K^\pm mesons. However, since the fit of strange meson spectra was not quite satisfactory (particularly in the case of flavor independent Gross-Neveu coupling), no such attempt will be made in this work.

IV. SUMMARY

We have considered the collinear model for QCD where all modes with nonzero transverse momentum (relative to an arbitrary, but fixed, direction) are neglected. Such a model has not been derived from QCD, and should thus be regarded as a purely phenomenological model. Within this model, we focussed on the limit where the effective mass of the transverse gluon becomes very large, but with an appropriately rescaled coupling to the quarks. As a result, one obtains a model that resembles the 't Hooft model but with helicity degrees of freedom for the quarks and point-like helicity-dependent quark-antiquark interactions that resemble the chiral Gross-Neveu model. This limiting case of collinear QCD is solvable for large N_C .

Given the ad-hoc truncation of the degrees of freedom, one would be tempted to dismiss such a model as not being a very useful model for QCD_{3+1} . However, as the physical observables presented in this paper indicate, the model yields a remarkably good description for many experimental data.

First of all, the spectrum of vector and axial-vector mesons turns out to be rotational invariant (i.e. helicity independent!).

Secondly, with only three free parameters available [which are fixed to reproduce the π , ρ and $\rho(1450)$ masses] one obtains an extraordinarily good result for the masses of other non-strange mesons. One of the most surprising result in the calculations of the spectrum was the excellent agreement with the mass of the $a_0(980)$, which is often difficult in quark models and which is believed to possess a large $K\bar{K}$ component (which is not there at large N_C). We have no explanation for this surprisingly good agreement of the model results with the experimental data. This agreement might be accidental and it does also depend on which physical mesons are identified with meson states within the model. Since the model lacks transverse momenta, the model contains of course much less states than for example the quark model and therefore one must pick a subset of states with which the model states are identified. While the choice made in the paper seemed by far the most reasonable, there is

some uncertainty in the assignment of quantum numbers since the model lacks full rotational invariance.

The spectra of mesons containing strange quarks, were less well reproduced. If one uses the same coupling in the strange and non-strange sectors, then it turns out to be impossible to fit the K and K^* masses at the same time. While the fit improves considerably, when one allows the Gross-Neveu coupling for strange quarks to differ from the coupling for light quarks, the overall fit for mesons with strange quarks never reaches the quality of the fit for non-strange mesons. Specifically, the $J^P = 0^+$ meson is not very well reproduced, which might be a hint that the agreement in the non-strange sector is to some extend accidental.

Motivated by the success of the meson spectrum calculations, we considered other observables as well. An observable which is particularly easily accessible in the LF framework are the LF wave functions of hadrons. The wave function for the π turned out to be almost completely flat [$\phi_\pi(x) = 1$ in the chiral limit]. In contrast, the wave function of the ρ turned out to be strongly peaked in the middle, which is more reminiscent of a weakly bound state. Physically, this difference did arise because the model has an attractive zero-range interaction which acts only in the π channel. A similar picture arises when one considers the LF wave functions for the a_0 and b_1 mesons. Both wave functions have nodes in the middle, which reflects the parity of these mesons, but only the wave function for the a_0 is non-vanishing at the boundary.

Despite the differences in their LF wave functions, the ρ and π meson turn out to have almost the same rms radius (i.e. slope of the vector form factor). The main reason for this result is vector meson dominance for the vector form factor at small momentum transfers, which is also a feature of collinear QCD. At large momentum transfers, the ρ form factor falls off much faster than the π form factor. Roughly speaking, a flat LF wave function corresponds to an equal time wave function which has a very large high momentum component (the end points of the LF wave function correspond to infinite momenta for the constituents in an equal time framework) thus resulting in less wave function suppression for the large momentum transfer form factor.

ACKNOWLEDGMENTS

The author thanks Craig Roberts and Eric Swanson for helpful comments and references. This work was supported by the D.O.E. (grant no. DE-FG03-96ER40965) and in part by TJNAF.

APPENDIX A: ON THE RENORMALIZATION OF THE VERTEX MASS

As long as the same cutoffs are used in a covariant calculation and in a LF calculation¹², the current quark mass of the covariant calculation and the vertex mass of the LF calculation usually are the same. Chiral symmetry breaking manifests itself through the renormalization of the kinetic mass term in the LF calculation [17–20].

The situation changes when the LF calculation is done using a Tamm-Dancoff approximation. This fact is best illustrated by considering a concrete example, such as a fermion interacting with some boson field. For simplicity, let us assume that the fermion self-energy has only a scalar piece and let us furthermore assume that this scalar piece is momentum independent¹³ — in other words, let us assume that

$$\Sigma(p) = \delta m, \quad (\text{A1})$$

where δm is a constant.

Without truncations of the Fock space, the three point interaction for the physical fermion (=solution to the Hamiltonian) gets modified through Feynman diagrams that include self-energies connected to the vertex by an instantaneous fermion line (Fig. 6).

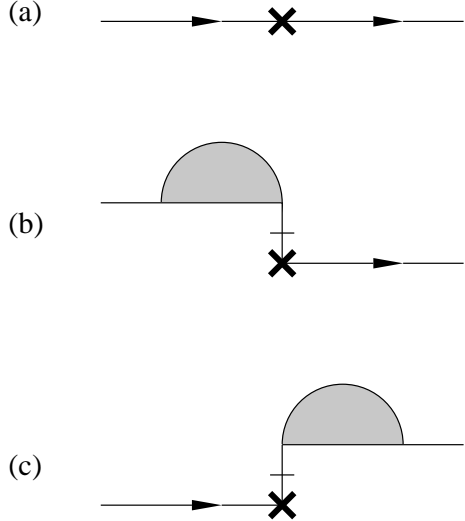


FIG. 6. Diagrams contributing to the three-point vertex for a physical fermion. (a) bare vertex, (b) self-energy insertion on the outgoing fermion line, (c) self energy insertion on the incoming fermion line.

¹²Under these circumstances, the only difference between a covariant calculation and a LF calculation is that zero-modes are omitted in the latter.

¹³An explicit model with such features is provided by a model where the boson mass goes to infinity and where the coupling is rescaled such that a nontrivial mass renormalization remains.

Note that under the above assumptions about the self-energy Σ , there are no further diagrams contributing to the physical vertex.

For the case of a (transverse) vector vertex¹⁴, the bare vertex yields a matrix element for helicity flip transitions

$$\Gamma_{\text{bare}}^{\text{flip}} = \frac{m_V^0}{\sqrt{q^+}} \left(\frac{1}{p^+} - \frac{1}{p'^+} \right), \quad (\text{A2})$$

where $q^+ = p^+ - p'^+$ is the momentum transfer at the vertex. The two diagrams with a self energy insertion in the incoming and outgoing external lines yield, respectively

$$\begin{aligned} \delta\Gamma_{\text{in}}^{\text{flip}} &= \frac{\delta m}{\sqrt{q^+}} \frac{1}{p^+} \\ \delta\Gamma_{\text{out}}^{\text{flip}} &= -\frac{\delta m}{\sqrt{q^+}} \frac{1}{p'^+}, \end{aligned} \quad (\text{A3})$$

so that

$$\begin{aligned} \Gamma^{\text{flip}} &\equiv \Gamma_{\text{bare}}^{\text{flip}} + \delta\Gamma_{\text{in}}^{\text{flip}} + \delta\Gamma_{\text{out}}^{\text{flip}} \\ &= \frac{m_V^0 + \delta m}{\sqrt{q^+}} \left(\frac{1}{p^+} - \frac{1}{p'^+} \right). \end{aligned} \quad (\text{A4})$$

This example shows that, if one imposes a Tamm-Dancoff (TD) truncation such that the δm correction to the vertex can no longer be generated through higher order Fock

¹⁴Other cases are analogous.

components, then one needs to renormalize the vertex mass accordingly in order to obtain the same physical results as without the TD truncation. Hence, with a TD approximation in place, the numerical value of the vertex mass need no longer agree with the numerical value of the current mass. In particular with a TD approximation, there is no reason that the vertex mass should vanish in the chiral limit. This is in contradistinction to LF calculations without TD approximations [18].

APPENDIX B: THE 'T HOOFT – GROSS – NEVEU MODEL

Because the Gross-Neveu interaction is quadratic in the non-dynamical component of the fermion field ψ_- , the constraint equation becomes non-linear and a canonical LF formulation of models with such an interaction is somewhere between difficult and impossible. Usually, one has to use some indirect methods for solution. In this Appendix, we will use covariant methods, supplemented by the LF solution to QCD_{1+1} , to construct a solution to the Gross-Neveu model with additional QCD_{1+1} interactions.

Let us consider the 1+1 dimensional model

$$\mathcal{L} = \bar{\psi} \left(i\partial - \frac{G}{\sqrt{N}} A - m \right) \psi - \frac{1}{2} \text{tr} (F_{\mu\nu} F^{\mu\nu}) - \frac{\gamma}{2N} \left[(\bar{\psi} \psi)^2 - (\bar{\psi} i\gamma_5 \psi)^2 \right], \quad (\text{B1})$$

where ψ has N color components (fundamental representation), $F_{\mu\nu} = \partial_\mu A_\nu - \partial_\nu A_\mu + i \frac{G}{\sqrt{N}} [A_\mu, A_\nu]$ is the gauge field and the limit $N \rightarrow \infty$ is implied. Obviously, for $\gamma = 0$ one obtains the 't Hooft model (QCD_{1+1} in the limit $N \rightarrow \infty$) [10], while for $G = 0$ the model reduces to the chiral Gross-Neveu model [11]. Because of the four fermion interaction, \mathcal{L} has to be renormalized.¹⁵

Before we derive the bound state equation corresponding to Eq. (B1), let us illustrate the techniques in the simpler case $G = 0$ (the chiral Gross-Neveu model): First of all, the scalar tadpole gives rise to a “constituent mass” M for the fermion. Secondly, since we are considering the $N \rightarrow \infty$ limit, the meson spectrum can be determined by summing up a (geometric) series of bubbles, yielding for the pseudo-scalar two-point function¹⁶

$$D_\pi(p^2) = \left(\frac{1}{\gamma} - i \int \frac{d^2 q}{(2\pi)^2} \text{tr} \frac{1}{(q-M)(q-p-M)} \right)^{-1}. \quad (\text{B2})$$

The integral in Eq. (B2) diverges logarithmically. We renormalize by subtracting at $p^2 = 0$ (strictly speaking we first introduce a regulator, then subtract and then send the regulator to infinity), yielding

$$D_\pi(p^2) = \left(\frac{1}{\gamma_{ren}} - \frac{1}{2\pi} \int_0^1 dx \frac{p^2}{M^2 - p^2 x(1-x)} \right)^{-1}, \quad (\text{B3})$$

where the renormalized (finite!) coupling is related to the bare coupling (zero!) via (cut-offs not explicitly shown)

$$\begin{aligned} \frac{1}{\gamma_{ren}} &= \frac{1}{\gamma} - i \int \frac{d^2 q}{(2\pi)^2} \text{tr} \frac{1}{(q-M)(q-M)} \\ &= \frac{1}{\gamma} - \frac{1}{2\pi} \int_0^1 \frac{dx}{x(1-x)}. \end{aligned} \quad (\text{B4})$$

The pseudo-scalar bound state (in the following referred to as the pion) mass is obtained in terms of the renormalized coupling by searching the pole of $D_\pi(p^2)$. In practice, one often turns the argument around and uses the pion mass as an input parameter, which yields the renormalized coupling as a function of the pion mass

$$0 \stackrel{!}{=} \frac{1}{\gamma_{ren}} - \frac{1}{2\pi} \int_0^1 dx \frac{\mu_\pi^2}{M^2 - \mu_\pi^2 x(1-x)}. \quad (\text{B5})$$

Since the 't Hooft model is most conveniently solved in the LF framework, we will also formulate the 't Hooft – Gross – Neveu model using LF quantization. As a warmup exercise, we thus reconsider the Gross-Neveu model in this framework as well. Using standard canonical quantization plus renormalization of the kinetic mass plus (as explained in Appendix A) renormalization of the vertex mass one finds the (still ill defined!) bound state equation for pseudo-scalar mesons

$$\mu^2 \psi(x) = \frac{M^2 \psi(x)}{x(1-x)} - \frac{\gamma M^2}{x(1-x)} \int \frac{dy}{2\pi} \frac{\psi(y)}{y(1-y)} \quad (\text{B6})$$

(for scalar mesons, where the wave-function is odd under $x \rightarrow 1 - x$, another term contributes which is omitted here for simplicity). Note that we set the vertex mass equal to the kinetic mass in Eq. (B6). As is explained in Appendix A, the vertex mass can acquire nontrivial renormalization, if certain corrections are suppressed by the approximations used (here: fermion tadpoles connected to the bare vertex by an instantaneous fermion line). The fact that we set it here equal to the kinetic mass term is arbitrary and irrelevant, since the interaction term is also multiplied by the (still undetermined) bare coupling constant. But, in order to achieve maximum similarity with the covariant approach, we set the vertex mass equal to the kinetic mass at this point.

Eq. (B6) yields a divergent solution, since $\psi(x) \xrightarrow{x \rightarrow 0, 1} \text{const.}$ and thus $\int dy \psi(y)/y(1-y)$ diverges. This divergence is exactly the same divergence that one obtains in

¹⁵We closely follow Ref. [12], where more details can be found.

¹⁶Up to an overall normalization factor, which is not relevant for determining bound state masses.

the covariant approach as well (before coupling constant renormalization) as one can see by reducing Eq. (B2) to a parameter integral, yielding

$$D_\pi(p^2) = \left(\frac{1}{\gamma} - \frac{1}{2\pi} \int_0^1 \frac{dx}{x(1-x)} \frac{M^2}{M^2 - p^2 x(1-x)} \right)^{-1} \quad (B7)$$

and the whole divergence can be avoided provided one renormalizes properly. Here we will use a trick¹⁷ to arrive at a renormalized bound state equation: the operator identity

$$\partial_\mu (\bar{\psi} \gamma^\mu \gamma_5 \psi) = 2m \bar{\psi} i \gamma_5 \psi, \quad (B8)$$

where m is the current quark mass, together with Lorentz covariance, implies for vacuum to meson (on shell) matrix elements

$$p^- \langle 0 | \bar{\psi} \gamma^+ \gamma_5 \psi | n, p \rangle = m \langle 0 | \bar{\psi} \gamma_5 \psi | n, p \rangle, \quad (B9)$$

i.e. in terms of the wave-function

$$\mu_n^2 \int_0^1 dx \psi_n(x) = m \int_0^1 dx \frac{M}{x(1-x)} \psi_n(x) \quad (B10)$$

The reason M and not m appears in the LF expression for $\langle 0 | \bar{\psi} i \gamma_5 \psi | \pi(p) \rangle$ is again the Tamm-Dancoff expansion used. We can use this identity to express the divergent integral in Eq. (B6) by a convergent integral, yielding the renormalized (but non-hermitian, since the Hamiltonian depends on the eigenvalue) bound state equation for the pion channel

$$\mu^2 \psi(x) = \frac{M^2 \psi(x)}{x(1-x)} - \frac{\gamma M \mu^2}{mx(1-x)} \int \frac{dy}{2\pi} \psi(y). \quad (B11)$$

This ‘miracle’ is possible since the current quark mass itself is cutoff dependent and goes to zero (for fixed physical masses) as the cutoff is sent to infinity. In fact, it goes to zero in such a way that the ratio γ/m stays finite, which motivates the definition

$$\gamma_{ren}^{LF} \equiv \frac{\gamma M}{m}. \quad (B12)$$

A consistency check of this result is obtained by explicitly solving the renormalized integral equation. From Eq. (B11) one finds

$$\psi(x) = \frac{\gamma_{ren}^{LF} \mu^2}{M^2 - x(1-x)\mu^2} \int \frac{dy}{2\pi} \psi(y). \quad (B13)$$

Consistency requires that

$$1 = \gamma_{ren}^{LF} \mu^2 \int_0^1 \frac{dx}{2\pi} \frac{1}{M^2 - x(1-x)\mu^2}, \quad (B14)$$

which we recognize as the pole condition for $D_\pi(p^2)$ [Eq. (B3)] with γ_{ren} replaced by γ_{ren}^{LF} .

Let us now proceed to the full ‘t Hooft – Gross -Neveu model (B1). A calculation analogous to the covariant procedure discussed above can again be obtained by summing up a chain of pseudo-scalar bubbles, but now each bubbles is dressed by the QCD_{1+1} interactions as well as by the Gross – Neveu (tadpole) self-energy.¹⁸

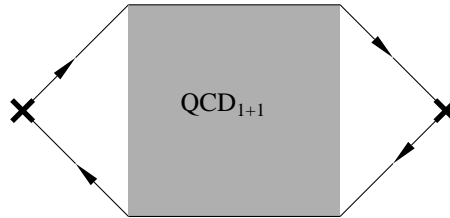


FIG. 7. In the pseudo-scalar two-point function, the $q\bar{q}$ propagation within each bubble is governed by the QCD_{1+1} Kernel in planar approximation (\rightarrow ‘t Hooft model).

In practice, these bubbles can be evaluated by inserting a complete set of (‘t Hooft-) meson states

$$D_\pi^{-1}(p^2) = \frac{1}{\gamma} - \frac{1}{2\pi} \sum_n \frac{g_P(n)^2}{\tilde{\mu}_n^2 - p^2}, \quad (B15)$$

where the $\tilde{\mu}_n$ and $g_P(n)$ are the masses and pseudo-scalar couplings of the n -th meson solution for the ‘t Hooft equation. The masses are most conveniently calculated in terms of the LF wave-functions

$$g_P(n) = M \int_0^1 dx \left(\frac{1}{x} + \frac{1}{1-x} \right) \psi_n(x). \quad (B16)$$

The sum in Eq. (B15) diverges, but since QCD_{1+1} is superrenormalizable, this is only the free field divergence. We renormalize again by performing a zero momentum subtraction, yielding

$$D_\pi^{-1}(p^2) = \frac{1}{\gamma_{ren}} - \frac{1}{2\pi} \sum_n \frac{p^2 g_P(n)^2}{\tilde{\mu}_n^2 (\tilde{\mu}_n^2 - p^2)}, \quad (B17)$$

where

¹⁷A similar trick has been used by T. Heinzl (talk given at the ‘1997 workshop on LF quantization’ in Les Houches, France).

¹⁸The fact that the fermion lines within the Gross – Neveu tadpoles are dressed by QCD_{1+1} interactions only changes the self-mass by a finite amount. Since the induced mass is only a bare parameter anyway, this additional renormalization of a parameter that is already renormalized has no further consequences.

$$\frac{1}{\gamma_{ren}} = \frac{1}{\gamma} - \sum_n \frac{g_P(n)^2}{\tilde{\mu}_n^2} \quad (B18)$$

is finite. For the scalar channel we are *not* free to renormalize independently, since chiral symmetry demands that the scalar and pseudo-scalar couplings are the same. This yields

$$\begin{aligned} D_\sigma^{-1}(p^2) &= \frac{1}{\gamma} - \frac{1}{2\pi} \sum_n \frac{g_S(n)^2}{\tilde{\mu}_n^2 - p^2} \\ &= \frac{1}{\gamma_{ren}^S} - \frac{1}{2\pi} \sum_n \frac{p^2 g_S(n)^2}{\tilde{\mu}_n^2 (\tilde{\mu}_n^2 - p^2)}, \end{aligned} \quad (B19)$$

where

$$g_S(n) = M \int_0^1 dx \left(\frac{1}{x} - \frac{1}{1-x} \right) \psi_n(x) \quad (B20)$$

are the scalar couplings and

$$\frac{1}{\gamma_{ren}^S} = \frac{1}{\gamma_{ren}^P} + \frac{1}{2\pi} \sum_n \frac{g_S(n)^2 - g_P(n)^2}{\tilde{\mu}_n^2} \quad (B21)$$

accounts for the (finite) differences in the zero momentum subtraction in the scalar and pseudo-scalar channels. For practical calculations, the following representation is also useful

$$D_\sigma^{-1}(p^2) = D_\pi^{-1}(p^2) + \frac{1}{2\pi} \sum_n \frac{g_S(n)^2 - g_P(n)^2}{\mu_n^2} \quad (B22)$$

Eqs. (B17) and (B19) or (B22) are perfectly suitable for a numerical determination of the spectrum of the 't Hooft – Gross – Neveu model. However, since we want to determine LF wave-functions and parton distribution functions, we also need to understand how to renormalize the LF wave equation for this model. The canonical procedure (modulo renormalization of both kinetic and vertex masses as explained above) yields the (still ill defined) LF bound state equation for this model

$$\begin{aligned} \mu^2 \psi(x) &= \frac{M^2 \psi(x)}{x(1-x)} + \int_0^1 dy \frac{\psi(x) - \psi(y)}{(x-y)^2} \\ &\quad - \frac{\gamma M^2}{x(1-x)} \int_0^1 \frac{dy}{2\pi} \frac{\psi(y)}{y(1-y)} \\ &\quad - \frac{\gamma M^2(1-2x)}{x(1-x)} \int_0^1 \frac{dy}{2\pi} \frac{(1-2y)\psi(y)}{y(1-y)}. \end{aligned} \quad (B23)$$

In the pseudo-scalar channel, we can use the same procedure that we introduced in connection with the Gross – Neveu model, namely replacing the pseudo-scalar coupling by the vector coupling, which yields the renormalized LF bound state equation for the 't Hooft – Gross – Neveu model in the pseudo-scalar channel (i.e. only even wave functions)

$$\begin{aligned} \mu^2 \psi(x) &= \frac{M^2 \psi(x)}{x(1-x)} + G^2 \int_0^1 dy \frac{\psi(x) - \psi(y)}{(x-y)^2} \\ &\quad - \frac{\gamma_{ren}^{LF} M^2 \mu^2}{x(1-x)} \int_0^1 \frac{dy}{2\pi} \psi(y). \end{aligned} \quad (B24)$$

It is quite easy to verify consistency of the renormalized LF equation (B24) with the more conventionally obtained result (B17). Using the Green's function for the 't Hooft equation,

$$G(x, y, p^2) \equiv \sum_n \frac{\psi_n(x) \psi_n(y)}{\tilde{\mu}_n^2 - p^2}, \quad (B25)$$

one can rewrite Eq. (B24) in the form

$$\psi(x) = \int_0^1 dy G(x, y, \mu^2) \frac{\gamma_{ren}^{LF} M^2}{y(1-y)} \int_0^1 \frac{dz}{2\pi} \psi(z). \quad (B26)$$

Upon integrating over x and using the fact that the solutions to 't Hooft's equation satisfy

$$\tilde{\mu}_n^2 \int_0^1 dx \psi_n(x) = M^2 \int_0^1 dx \frac{\psi_n(x)}{x(1-x)} \quad (B27)$$

we recover Eq. (B17) — provided we identify γ_{ren}^{LF} with γ_{ren} .

For scalar mesons, we have not been able to derive a renormalized LF bound state equation. However, this does not prevent us from calculating the LF wave functions of scalar resonances, using the following trick:¹⁹ From Eq. (B23) one notes that the wave functions for scalar states satisfy

$$\psi_n(x) \propto \int_0^1 dy G(x, y, \mu_n^2) \left(\frac{M}{x} - \frac{M}{1-x} \right), \quad (B28)$$

where M_n^2 is the invariant mass of the bound state. Thus one can first obtain the bound state mass from the poles of $D_\sigma(p^2)$ [i.e. from Eq. (B22)] and then one determines $\psi_n(x)$ (up to a normalization factor) by solving the linear equation corresponding to Eq. (B28), i.e. one solves

$$(\mu_\sigma^2 - H_{th}) \psi = M \left(\frac{1}{x} - \frac{1}{1-x} \right) \quad (B29)$$

for $\psi(x)$, where H_{th} is the 't Hooft Hamiltonian.

[1] S. J. Brodsky and D. G. Robertson, proceedings of ELFE Summer School on Confinement Physics, Cambridge, England, 22-28 Jul 1995, e-Print archive: hep-ph/9511374.

¹⁹We demonstrate this trick only for scalar meson but it works analogously for pseudo-scalar mesons.

- [2] S.J. Brodsky et al., Part. World **3**, 109 (1993).
- [3] K. G. Wilson et al., Phys. Rev. D **49**, 6720 (1994).
- [4] R. J. Perry, invited lectures presented at ‘Hadrons 94’, Gramado, Brazil, April 1994, e-Print archive: hep-ph/9407056.
- [5] M. Burkardt, Advances Nucl. Phys. **23**, 1 (1996).
- [6] F. Antonuccio and S. Dalley, Nucl. Phys. B **461**, 275 (1996); B. vande Sande and M. Burkardt, Phys. Rev. D **53**, 4628 (1996).
- [7] F. Antonuccio and S. Dalley, Phys. Lett. B **376**, 154 (1996); S. Dalley, talk at “New Nonperturbative Methods and Quantization of the Light Cone”, Les Houches, France, Feb 1997, e-Print archive: hep-th/9704211.
- [8] H.-C. Pauli and S. J. Brodsky, Phys. Rev. D **32**, 1993 (1985); *ibid* 2001 (1985).
- [9] B. vande Sande, Phys. Rev. D **54**, 6347 (1996).
- [10] G. ’t Hooft, Nucl. Phys. B **75**, 461 (1974).
- [11] D.J. Gross and A. Neveu, Phys. Rev. D **10**, 3235 (1974).
- [12] B. Rosenstein, B.J. Warr and S.H. Park, Phys. Rep. **205**, 59 (1991).
- [13] M.B. Einhorn, Phys. Rev. D **14**, 3451 (1976).
- [14] R.M. Barnett, *et al.*, Phys. Rev. D **54**, 1 (1996).
- [15] S.R. Amendolia, *et al.*, Nucl. Phys. B **277**, 168 (1986); C.N. Brown, *et al.*, Phys. Rev. D **8**, 92 (1973); C.J. Bebek, *et al.*, Phys. Rev. D **13**, 25 (1976); C.J. Bebek, *et al.*, Phys. Rev. D **17**, 1693 (1976).
- [16] T. Barnes et al., Phys. Rev. D **55**, 4157 (1997).
- [17] M. Burkardt, Phys. Rev. D **54**, 2913 (1996).
- [18] M. Burkardt and H. El-Khozondar, to appear in Phys. Rev. D (May15, 1996), e-Print archive: hep-ph/9609250.
- [19] M. Burkardt, lecture notes, International School on Light-Front Quantization and Non-Perturbative QCD , Ames, IA, May 1996, e-Print archive: hep-ph/9611416.
- [20] M. Burkardt, submitted to Phys. Rev. D, e-Print archive: hep-th/9704162.